

Semihadronic and hadronic decays of ρ^0 and ω mesons coherently photoproduced in the isoscalar nuclei

Swapan Das ¹

*Nuclear Physics Division, Bhabha Atomic Research Centre
Mumbai-400085, India*

Abstract

The interference of the ρ^0 and ω mesons has been studied in the hadronic and leptonic decay channels, i.e., dipion and dilepton decay channels respectively, but this interference is not studied yet in the semihadronic or semileptonic decay channel, e.g., $V \rightarrow \pi^0\gamma$. V denotes either ρ^0 or ω meson. To look for the quoted interference in the $\pi^0\gamma$ decay channel as well as the contribution of ρ meson to the cross section, the correlated $\pi^0\gamma$ invariant mass distribution spectra are calculated in the photonuclear reaction in the multi-GeV region. It is assumed that these bosons arise in the final state due to the decay of ρ^0 and ω mesons which are photoproduced coherently in the isoscalar nucleus. The elementary reaction in the nucleus is considered to proceed as $\gamma N \rightarrow VN$; $V \rightarrow \pi^0\gamma$. The forward propagation of the ρ and ω mesons and the near forward emission of pion are considered, so that they can be described by the eikonal form. The meson nucleus interactions are evaluated using $t\rho$ approximation. Replacing the decay vertex $V \rightarrow \pi^0\gamma$ by $V \rightarrow \pi^+\pi^-$ in the above formalism, it is also used to study the $\rho - \omega$ interference in the $\pi^+\pi^-$ decay channel.

Keywords: photonuclear reaction, $\rho - \omega$ interference, meson nucleus potential
PACS number(s): 25.20.-x, 13.60.Le, 13.20.-v

1 Introduction

It is well known that the dipion (i.e., $\pi^+\pi^-$) and dilepton (e.g., e^+e^- , $\mu^+\mu^-$, ... etc.) emission in the reactions (multi-GeV region) occur because of the decay of ρ^0 and ω mesons, produced in the intermediate state of the reactions. The data of these reactions are described better because of the interference of ρ and ω mesons [1]. The $e^+e^- \rightarrow \pi^+\pi^-$ reaction has been understood as $e^+e^- \rightarrow \gamma \rightarrow V \rightarrow \pi^+\pi^-$ [2] (see the references there in). The symbol V is used to describe the vector meson, i.e., either ρ^0 or ω meson, throughout the text. Though the dominant contribution to the cross section of the $e^+e^- \rightarrow \pi^+\pi^-$ reaction arises due to the ρ meson, the data are better reproduced because of the inclusion

¹email: swapand@barc.gov.in

of ω meson contribution to the reaction. The ρ – ω mixing parameter and pion form factor [2] have been described well in the study of this reaction.

The distinct ρ – ω interference has also been seen in the dilepton production in the photonuclear reaction in the multi-GeV region [3, 4]: $\gamma A \rightarrow VA$; $V \rightarrow e^+e^-$. Various quantities, such as γ – V coupling constant, the relative phase between the ρ and ω mesons production, ... etc., have been extracted from the study of this reaction. The ρ – ω interference was also studied in the e^+e^- production (due to the decay of the vector mesons produced near threshold) in the photo-induced reaction on nucleon [5]. Recently, the measurement on the dilepton emission was reported from JLab to the search the quoted interference in the γ proton reaction [6]. To be mentioned, the ρ^0 meson photo-produced in the multi-GeV nuclear reaction was detected by the $\pi^+\pi^-$ [7] since the decay branching ratio of $\rho^0 \rightarrow \pi^+\pi^-$ is $\sim 100\%$. Though the branching ratio of ω meson to the $\pi^+\pi^-$ decay channel is very small compared to that of ρ^0 meson, the ρ – ω interference is also visible in the $\pi^+\pi^-$ photoproduction reaction on nuclei [8, 9, 10].

It must be mentioned that the ρ – ω interference has been well studied in the hadronic and leptonic decay channels but it is not yet done for the semi-hadronic (or semi-leptonic) decay channels, i.e., $V \rightarrow \pi^0\gamma$ for example. Recent past, the correlated $\pi^0\gamma$ emission (in the GeV region) was studied in the photonuclear reaction to investigate the modification of ω meson in the nucleus [11]. However, the contribution of ρ meson to this reaction is never incorporated because (as shown latter) it is too small in the ω meson peak region.

As stated earlier, the contribution of ω meson to the $\pi^+\pi^-$ production in the e^+e^- and γA reactions is negligibly small (compared to that of ρ^0 meson) but the data are better reproduced due to the ρ – ω interference [2, 9]. In fact, this would have never been known unless the contribution of ω meson included in the calculation. Therefore, the contribution of ρ meson to the $\pi^0\gamma$ production reaction should be studied so that the change in the cross section of the reaction because of the ρ meson (and ρ – ω interference) can be recorded. To disentangle it, both ρ^0 and ω mesons are included in the calculation for the cross section of the $\pi^0\gamma$ invariant mass distribution in the photonuclear reaction, i.e., the π^0 and γ bosons in the final state are considered to arise due to the decay of both ρ^0 and ω mesons produced coherently in the intermediate state of the reaction. The elementary reaction occurring in the nucleus is assumed to proceed as $\gamma N \rightarrow VN$; $V \rightarrow \pi^0\gamma$, where V denotes the vector meson (i.e., ρ or ω meson, as mentioned earlier).

The forward production of the vector meson in the reaction is considered since it ensures the coherence of its production amplitude in a nucleus [4, 8]. The emission of pion is also considered near forward direction. Both the vector meson propagator and the pion distorted wave function are expressed by the eikonal form. The meson nucleus interaction (optical potential) is evaluated using $t\rho$ approximation. The isoscalar nuclei are consider in the reaction so that one pion exchange contribution to the vector meson (specifically, ω meson) production in the nucleus can be ignored [4, 8]. Considering the

decay channel $V \rightarrow \pi^+\pi^-$ instead of $V \rightarrow \pi^0\gamma$ in the reaction mechanism stated above, it can be used to describe the $\pi^+\pi^-$ emission due to the decay of the vector meson produced coherently in the photonuclear reaction. Therefore, the formalism is developed to calculate the cross section for both $\pi^0\gamma$ and $\pi^+\pi^-$ invariant mass distribution spectrum in the quoted reaction.

2 Formalism

The $(\gamma, V \rightarrow ab)$ reaction on a nucleus consists of three parts: (i) the vector meson V photoproduction in the nucleus, (ii) the propagation of this meson through the nucleus, and (iii) the decay of vector meson V into ab (i.e., $V \rightarrow ab$) in the final state, where ab represents either $\pi^0\gamma$ or $\pi^+\pi^-$. The first part can be described by the generalized potential or self-energy of the vector meson in a nucleus [12], i.e.,

$$\Pi_{\gamma A \rightarrow V A}(\mathbf{r}) = K \tilde{f}_{\gamma N \rightarrow V N}(0) \varrho(\mathbf{r}), \quad (1)$$

with $K = -4\pi E_V(1/\tilde{E}_V + 1/\tilde{E}_N)$. $\tilde{f}_{\gamma N \rightarrow V N}$ is the amplitude of the elementary reaction: $\gamma N \rightarrow V N$. The symbol “*tilde*” on the quantities denote those in the γN cm system. $\varrho(\mathbf{r})$ represents the matter density distribution of the nucleus. As mentioned earlier, one pion exchange contribution can be neglected for the vector meson production in the isoscalar nucleus [4, 8].

The propagator of the vector meson can be expressed as $(-g_\nu^\mu + \frac{1}{m_V^2} k_V^\mu k_{V,\nu})G_V(m; \mathbf{r} - \mathbf{r}')$ [11, 13], where the scalar part of it, i.e., $G_V(m, \mathbf{r} - \mathbf{r}')$, describes the propagation of this meson from its production point \mathbf{r} to decay point \mathbf{r}' . For the forward going vector meson, $G_V(m, \mathbf{r} - \mathbf{r}')$ can be well described by the eikonal form, i.e.,

$$G_V(m; \mathbf{r} - \mathbf{r}') = \delta(\mathbf{b} - \mathbf{b}')\theta(z' - z)e^{i\mathbf{k}_V \cdot (\mathbf{r} - \mathbf{r}')} D_{\mathbf{k}_V}(m; \mathbf{b}, z', z). \quad (2)$$

The factor $D_{\mathbf{k}_V}(m; \mathbf{b}, z', z)$ in this equation carries the information about the nuclear effect on the vector meson during its propagation through the nucleus, since it involves the vector meson nucleus optical potential V_{OV} . The expression for $D_{\mathbf{k}_V}(m; \mathbf{b}, z', z)$ is

$$D_{\mathbf{k}_V}(m; \mathbf{b}, z', z) = -\frac{i}{2k_{V\parallel}} \exp \left[\frac{i}{2k_{V\parallel}} \int_z^{z'} dz'' \{ \tilde{G}_{0V}^{-1}(m) - 2E_V V_{OV}(\mathbf{b}, z'') \} \right], \quad (3)$$

where $\tilde{G}_{0V}^{-1}(m) = m^2 - m_V^2 + im_V \Gamma_V(m)$ is the inverse of the free space vector meson propagator. m_V is the pole mass of this meson: $m_{\rho^0} = 775.26$ MeV and $m_\omega = 782.65$ MeV, listed in Ref. [14]. All other symbols carry their usual meanings.

The γ wave function is described by the plane wave associated with its polarization vector. As mentioned earlier, the particles ab in the final state (i.e., the decay products

of the vector meson) are considered either $\pi^+\gamma$ or $\pi^+\pi^-$. For the pion emission near the forward direction, the wave function for it can be written in eikonal form [11, 15], i.e.,

$$\chi^{(-)*}(\mathbf{k}_\pi, \mathbf{r}') = e^{-i\mathbf{k}_\pi \cdot \mathbf{r}'} D_{\mathbf{k}_\pi}^{(-)*}(\mathbf{b}, z'), \quad (4)$$

where $D_{\mathbf{k}_\pi}^{(-)*}(\mathbf{b}, z')$ denotes the distortion due to the pion nucleus interaction (i.e., pion nucleus optical potential $V_{O\pi}$). It is given by

$$D_{\mathbf{k}_\pi}^{(-)*}(\mathbf{b}, z') = \exp \left[-\frac{i}{v_{\pi\parallel}} \int_{z'}^{\infty} dz_j V_{O\pi}(\mathbf{b}, z_j) \right], \quad (5)$$

where v_π is the velocity of pion.

The T -matrix T_{fi} of the coherent ($\gamma, V \rightarrow ab$) reaction on a nucleus is related to its reduced matrix \mathcal{M}_{fi} as $T_{fi} = \frac{\mathcal{M}_{fi}}{\sqrt{(2E_\gamma 2E_a 2E_b)}}$, where \mathcal{M}_{fi} can be written as

$$\mathcal{M}_{fi} = \sum_{V=\rho^0, \omega} \Gamma_{Vab} F_{\gamma, V \rightarrow ab}. \quad (6)$$

Γ_{Vab} in this equation describes $V \rightarrow ab$ decay vertex. The Lagrangian for it is given latter. $F_{\gamma, V \rightarrow ab}$ represents the space part of \mathcal{M}_{fi} , i.e.,

$$F_{\gamma, V \rightarrow ab} = \langle ab | G_V(m; \mathbf{r} - \mathbf{r}') \Pi_{\gamma A \rightarrow V A}(\mathbf{r}) | \gamma \rangle. \quad (7)$$

$G_V(m; \mathbf{r} - \mathbf{r}')$ and the wave function for the particles a and b are given in Eqs. (2) and Eq. (4) respectively.

The cross section of the coherent ($\gamma, V \rightarrow ab$) reaction on a nucleus is given by

$$d\sigma = \frac{(2\pi)^4}{v_{\gamma A}} \delta^4(k_i - k_f) \langle |T_{fi}|^2 \rangle \Pi_{f(=a,b,A')} [d\mathbf{k}/(2\pi)^3]_f, \quad (8)$$

where $v_{\gamma A}$ is the relative velocity of the incident γ with respect to the target nucleus A , i.e., $v_{\gamma A} = |v_\gamma - v_A|$. The primed quantity, i.e., A' , denotes the recoil nucleus. The annular bracket around T_{fi} represents the average over initial states and the summation over final states.

3 Result and Discussions

The total decay width of the vector meson $\Gamma_V(m)$, appearing below Eq. (3), is composed of the partial widths of its various decay channels [14]: $\Gamma_{\rho^0}(m) = 99.94 \times 10^{-2} \Gamma_{\rho^0 \rightarrow \pi^+ \pi^-}(m) + 6.0 \times 10^{-4} \Gamma_{\rho^0 \rightarrow \pi^0 \gamma}(m)$, and $\Gamma_\omega(m) = 89.9 \times 10^{-2} \Gamma_{\omega \rightarrow \pi^+ \pi^- \pi^0}(m) + 8.5 \times 10^{-2} \Gamma_{\omega \rightarrow \pi^0 \gamma}(m) + 1.6 \times 10^{-2} \Gamma_{\omega \rightarrow \pi^+ \pi^-}(m)$. The partial decay widths are illustrated in Ref. [16].

The meson nucleus optical potentials V_{OM} (i.e., V_{OV} in Eq. (3) and $V_{O\pi}$ in Eq. (5)) are evaluated using $t\varrho$ approximation [15, 17]. According to it, V_{OM} is given by

$$V_{OM}(\mathbf{r}) = -\frac{v_M}{2}[i + \alpha_{MN}]\sigma_t^{MN}\varrho(\mathbf{r}), \quad (9)$$

where v_M is the velocity of the meson M . $\varrho(\mathbf{r})$ has been defined in Eq. (1). The scattering parameters α_{MN} and σ_t^{MN} denote the ratio of the real to imaginary part of the meson nucleon forward scattering amplitude $f_{MN}(0)$ and the meson nucleon total cross section respectively.

The imaginary part of f_{MN} for the vector meson is extracted from the data of the elementary $\gamma N \rightarrow VN$ reaction using vector meson dominance (VDM) model [18, 19, 20]. The typical values of σ_t^{VN} (in the considered energy region, i.e., 3-5 GeV) at $k_V = 4$ GeV/c are $\sigma_t^{\rho p} \simeq 35$ mb [18] and $\sigma_t^{\omega p} \simeq 40$ mb [20]. The real part of the ρ^0 meson nucleon scattering amplitude $f_{\rho N}$ is taken from the calculation of Kondratyuk et al., [18] which reproduce the data in the quoted energy region. For the ω meson nucleon scattering, $\alpha_{\omega N}$ have been calculated using additive quark model and Regge theory [19]: $\alpha_{\omega N} = \frac{0.173(s/s_0)^\epsilon - 2.726(s/s_0)^\eta}{1.359(s/s_0)^\epsilon + 3.164(s/s_0)^\eta}$, with $s_0 = 1$ GeV², $\epsilon = 0.08$ and $\eta = -0.45$. In fact, the vector meson dominance (VMD) model relates f_{MN} to $f_{\gamma N \rightarrow VN}$ (i.e., the vector meson photoproduction amplitude used in Eq. (1)) as $f_{\gamma N \rightarrow VN} = \frac{\sqrt{\pi}\alpha_{em}}{\gamma_V}f_{MN}$. α_{em} is the fine structure constant. γ_V is the photon to vector meson coupling constant as described in VMD model [21]. The values of γ_ρ and γ_ω , extracted from the measured width of $V \rightarrow e^+e^-$ [14], are 2.48 and 8.53 respectively [22]. For the pion nucleon scattering amplitude, the energy dependent experimentally determined values of $f_{\pi^\pm N}$ are listed in Ref. [23]. The π^0 meson nucleon scattering amplitude $f_{\pi^0 N}$ is estimated (using isospin algebra) as $f_{\pi^0 N} = \frac{1}{2}[f_{\pi^+ N} + f_{\pi^- N}]$. They are used to evaluate the pion nucleus optical potential.

The calculated ab (i.e., either $\pi^0\gamma$ or $\pi^+\pi^-$) invariant mass distribution spectra are presented afterwards in the figures, where the large-dashed curve represents the cross section due to ω meson. The cross section because of the ρ^0 meson is shown by the short-dashed curve. The dot-dashed curve arises because of the incoherent contribution of these mesons to the cross section of the reaction, i.e., the summation of the cross sections of the coherent ($\gamma, \rho^0 \rightarrow ab$) and ($\gamma, \omega \rightarrow ab$) reactions on the nucleus. The solid curve illustrates the coherently added cross sections of these reactions, i.e., the amplitudes of the reactions are added to get the cross section. The dot-dot-dashed curve shows the contribution to the cross section arising due to the $\rho - \omega$ interference.

3.1 $(\gamma, V \rightarrow \pi^0\gamma)$ reaction

The cross section for the $\pi^0\gamma$ invariant mass distribution in the coherent (γ, V) reaction on the isoscalar nuclei are calculated using the formalism (developed in the previous section)

where the particles a and b in the final state are replaced by π^0 and γ bosons respectively. The $V \rightarrow \pi^0\gamma$ decay is described by the Lagrangian [20, 24]:

$$\mathcal{L}_{V\pi\gamma} = \frac{f_{V\pi\gamma}}{m_\pi} \varepsilon_{\alpha\beta\delta\sigma} \partial^\alpha A^\beta \pi \cdot \partial^\delta \mathbf{V}^\sigma, \quad (10)$$

where $f_{V\pi\gamma}$ denotes the $V\pi\gamma$ coupling constant. The width of this decay [16] is given by

$$\Gamma_{V \rightarrow \pi^0 \gamma}(m) = \Gamma_{V \rightarrow \pi^0 \gamma}(m_V) \left[\frac{\tilde{k}(m)}{\tilde{k}(m_V)} \right]^3 \Theta(m - m_\pi), \quad (11)$$

where $\tilde{k}(m)$ is the momentum of the pion originating due to the vector meson of mass m decaying at rest. Since the final state interaction of the γ boson is negligible, $F_{\gamma, V \rightarrow ab}$ in Eq. (7) can be expressed as

$$F_{\gamma, V \rightarrow \pi^0 \gamma} = \int d\mathbf{r} \int_z^\infty dz' D_{\mathbf{k}_{\pi^0}}^{(-)*}(\mathbf{b}, z') D_{\mathbf{k}_V}(m; \mathbf{b}, z', z) e^{i(\mathbf{k}_\gamma - \mathbf{k}_V) \cdot \mathbf{r}} \Pi_{\gamma A \rightarrow V A}(\mathbf{r}). \quad (12)$$

The double differential cross section for the correlated $\pi^0\gamma$ invariant mass m distribution in the coherent ($\gamma, V \rightarrow \pi^0\gamma$) reaction on a nucleus, using Eq. (8), can be written as

$$\frac{d\sigma}{dm d\Omega_V} = P_{\pi^0\gamma} \left| \sum_{V=\rho^0, \omega} \Gamma_{V \rightarrow \pi^0\gamma}^{1/2}(m) F_{\gamma, V \rightarrow \pi^0\gamma} \right|^2, \quad (13)$$

where $P_{\pi^0\gamma}$ in this equation arises because of the phase-space of the reaction: $P_{\pi^0\gamma} = \frac{1}{(2\pi)^3} \frac{k_V^2 m^2 E_{A'}}{E_\gamma |k_V E_i - k_\gamma \cos\theta_V E_V|}$. $E_{A'}$ denotes the energy of the recoiling nucleus. The $\pi^0\gamma$ invariant mass distribution spectra are calculated for the fixed π^0 meson emission angle ($\theta_{\pi^0} = 1^\circ$) in the multi-GeV region. The bosons in the final state (i.e., π^0 and γ) arise due to the decay of the forward ($\theta_V = 0^\circ$) going vector meson (i.e., ρ^0 or ω meson) which is photoproduced coherently in the isoscalar nucleus.

The calculated $\pi^0\gamma$ invariant mass distribution spectra for ^{12}C nucleus (a isoscalar nucleus) are shown in Fig. 1. The beam energy E_γ is taken equal to 3 GeV. The density distribution $\varrho(\mathbf{r})$ of this nucleus is described by the Harmonic Oscillator Gaussian form [25], i.e.,

$$\varrho(\mathbf{r}) = \varrho_0 [1 + w(r/c)^2] e^{-(r/c)^2}; \quad (14)$$

with $w = 1.247$, $c = 1.649$ fm. Fig. 1 shows that the cross section at the peak due to ω meson (large-dashed curve) is distinctly largest. It appears at the pole mass of ω meson, i.e., $m \sim 0.78$ GeV. In this region, the cross section because of the ρ^0 meson (short-dashed curve) is negligibly small compared to the previous. The peak cross section, as shown in Fig. 1(a), is increased by $\approx 12\%$ because of the inclusion of the ρ^0 meson contribution in the calculated cross section.

It should be mentioned that the distinct $\rho^0 - \omega$ interference in the $\pi^+\pi^-$ and e^+e^- decay channels has been seen beyond the peak of the cross section [4, 9]. To explore that in the $\pi^0\gamma$ decay channel, the calculated cross section away from the peak region is presented in Fig. 1(b) for ^{12}C nucleus. The $\rho - \omega$ interference is distinctly visible in this figure in the regions of m below ($m < 0.76$ GeV) and beyond ($m > 0.80$ GeV) its value at the peak position. This figure also shows that the enhancement in the calculated cross section due to the inclusion of ρ meson in it (as shown in Fig. 1) is much larger than that occurs at the peak of the cross section, and the quoted enhancement increases as m is away from its value at the peak position. Fig. 1(b) shows that the contribution of ρ meson to the cross section is comparable to that of the ω meson at $m(\text{GeV}) \sim 0.64$ and 0.92 . In these regions of m , the calculated cross section is increased by $\sim 100\%$ due to the $\rho - \omega$ interference. In fact, the cross section is increased drastically (a factor of ~ 3.5) because of the ρ meson, resulting a remarkable change in the shape of $\pi^0\gamma$ invariant mass distribution spectrum in the regions few hundred MeV away from its peak.

To look for the contribution of the ρ^0 meson at higher energy, the $\pi^0\gamma$ invariant mass distribution spectra of the considered reaction are calculated at $E_\gamma = 5$ GeV. The calculated results, presented in Fig. 2, illustrates that the $\pi^0\gamma$ invariant mass m distribution spectra at 5 GeV are qualitatively similar to those at 3 GeV, see Fig. 1(b). The quoted interference and the change in the spectral shape (because of the ρ meson) in the region of m few hundred MeV away from its value at the peak position is also noticeable in this figure. The magnitude of the cross section is significantly increased with the beam energy. At the peak, it is enhanced by a factor of 3 due to the increase in the beam energy from 3 to 5 GeV. The cross section is increased from $47.3 \mu\text{b}/(\text{GeV sr})$ to $0.12 \text{ mb}/(\text{GeV sr})$ at $m = 0.64$ GeV, and it is increased from $59.52 \mu\text{b}/(\text{GeV sr})$ to $0.29 \text{ mb}/(\text{GeV sr})$ at $m = 0.92$ GeV because of the quoted enhancement in the beam energy.

Since large cross section away from the ω -meson peak region in the $\pi^0\gamma$ invariant mass distribution spectrum is preferable to study the $\rho - \omega$ interference, the heavy nucleus should be considered for it. Therefore, the cross section of the quoted reaction for ^{40}Ca (a heavier isoscalar nucleus) is calculated at 5 GeV. The density distribution $\varrho(\mathbf{r})$ of this nucleus can be described by 3-parameter Fermi distribution function [25]:

$$\varrho(\mathbf{r}) = \varrho_0 \frac{1 + w(r/c)^2}{1 + \exp[(r - c)/z]}; \quad (15)$$

with $w = -0.1017$, $c = 3.6685$ fm and $z = 0.5839$ fm [25]. The calculated spectra, as shown in Fig. 3, are qualitatively similar to those presented in the previous figures. The cross section for ^{40}Ca is significantly large compared to that for ^{12}C nucleus. As shown in this figure, the cross section at $m = 0.64$ GeV is $1.15 \text{ mb}/(\text{GeV sr})$ and it is $1.91 \text{ mb}/(\text{GeV sr})$ at $m = 0.92$ GeV.

The ratio of the amplitude of ρ^0 meson to that of the ω meson is given by $\xi =$

$\frac{\Gamma_{\rho \rightarrow \pi^0 \gamma}^{1/2} |F_{\gamma, \rho \rightarrow \pi^0 \gamma}|}{\Gamma_{\omega \rightarrow \pi^0 \gamma}^{1/2} |F_{\gamma, \omega \rightarrow \pi^0 \gamma}|}$, see Eq. (13). The value of ξ for ^{12}C nucleus (calculated at m_{ρ^0}) is $\simeq 1.17 \times 10^{-1}$ and the relative phase ϕ of these mesons is equal to 61° at $E_\gamma = 3$ GeV. At higher energy, i.e., $E_\gamma = 5$ GeV, the calculated values of ξ and ϕ for this nucleus are 1.24×10^{-1} and 63° where as those for ^{40}Ca nucleus are found equal to 1.28×10^{-1} and $\phi \simeq 61^\circ$.

3.2 $(\gamma, V \rightarrow \pi^+ \pi^-)$ reaction

The formalism already described is used to calculate the cross section for the $\pi^+ \pi^-$ invariant mass distribution spectra in the coherent (γ, V) reaction on the nucleus. In this reaction, the vector meson V decay products a and b (appearing in the formalism) are π^+ and π^- respectively. The Lagrangian, which describes $V \rightarrow \pi^+ \pi^-$ decay [21, 26], is given by

$$\mathcal{L}_{V\pi^+\pi^-} = g_{V\pi\pi} \mathbf{V}^\mu \cdot (\boldsymbol{\pi} \times \partial_\mu \boldsymbol{\pi}), \quad (16)$$

where $g_{V\pi\pi}$ denotes the $V\pi\pi$ coupling constant. The parameterized form of this decay width [16] can be written as

$$\Gamma_{V \rightarrow \pi^+ \pi^-}(m) = \Gamma_{V \rightarrow \pi^+ \pi^-}(m_V) \left(\frac{m_V}{m} \right) \left[\frac{\tilde{k}(m)}{\tilde{k}(m_V)} \right]^3 \Theta(m - 2m_\pi), \quad (17)$$

$\tilde{k}(m)$ is defined in Eq. (11). The form of $F_{\gamma, V \rightarrow ab}$ in Eq. (7) for $V \rightarrow \pi^+ \pi^-$ decay is given by

$$F_{\gamma, V \rightarrow \pi^+ \pi^-} = \int d\mathbf{r} \int_z^\infty dz' D_{\mathbf{k}_{\pi^+}}^{(-)*}(\mathbf{b}, z') D_{\mathbf{k}_{\pi^-}}^{(-)*}(\mathbf{b}, z') D_{\mathbf{k}_V}(m; \mathbf{b}, z', z) e^{i(\mathbf{k}_\gamma - \mathbf{k}_V) \cdot \mathbf{r}} \Pi_{\gamma A \rightarrow V A}(\mathbf{r}). \quad (18)$$

The double differential cross section $\frac{d\sigma}{dm dt}$ for the $\pi^+ \pi^-$ invariant mass m distribution of the considered reaction on ^{12}C nucleus is calculated to compare that with the data for the vector meson momentum $k_V = 6.4$ GeV and the transverse four-momentum transfer $t_T = -0.001$ GeV². The expression for $\frac{d\sigma}{dm dt}$, using Eq. (8), can be written as

$$\frac{d\sigma}{dm dt} = P_{\pi^+ \pi^-} \left| \sum_{V=\rho^0, \omega} m_V^{1/2} \Gamma_{V \rightarrow \pi^+ \pi^-}^{1/2}(m) F_{\gamma, V \rightarrow \pi^+ \pi^-} \right|^2, \quad (19)$$

with $P_{\pi^+ \pi^-} = \frac{\pi}{(2\pi)^3} \frac{k_V m E_{A'}}{E_\gamma^2 |k_V E_i - k_\gamma \cos \theta_V E_V|}$. The calculated ratio ξ of the amplitudes of ρ^0 and ω mesons and the relative phase ϕ of them are found equal to 8.66×10^{-2} and $\approx 65^\circ$ respectively. The measured $\pi^+ \pi^-$ invariant mass m distribution spectrum due to the decay of vector meson and backgrounds, taken from Ref. [10], are presented in Fig. 4.

The calculated spectra (added with the backgrounds) are also shown in this figure. The short-dashed curve represents the cross section due to ρ^0 meson. The solid curve arises because of the contribution of the ω meson coherently added to the previous. This figure shows that the calculated spectrum due to ρ meson is well accord with the data. The change in this spectrum due to the inclusion (coherently) of the ω meson contribution is insignificant except a sharp peak appears at the pole mass of this meson, i.e., $m_\omega = 782.65$ MeV.

It should be mentioned that the decay width $\Gamma_{\omega \rightarrow \pi^+\pi^-}(m_\omega)$, equal to 0.13 MeV, is negligibly small compared to $\Gamma_{\rho^0 \rightarrow \pi^+\pi^-}(m_{\rho^0})$, i.e., ~ 149 MeV. Therefore, a peak due to ω meson is not expected in the $\pi^+\pi^-$ invariant mass distribution spectrum. To explore the origin of the sharp peak appearing at the ω meson pole mass (i.e., $m = m_\omega$) in Fig. 4, the cross sections due to ρ^0 and ω mesons (along with their interference) are plotted in Fig. 5. This figure shows that the cross section due to ω meson (large-dashed curve) is negligibly small compared to that because of the ρ^0 meson (short-dashed curve) but the cross section due to the $\rho - \omega$ interference (dot-dot-dashed curve) is very much significant at $m = m_\omega$ in the $\pi^+\pi^-$ invariant mass distribution spectrum. Therefore, the sharp peak distinctly visible at the ω meson pole mass in Figs. 4 and 5 arises because of the quoted interference.

4 Conclusions

The $\rho - \omega$ interference is studied in the $\pi^0\gamma$ and $\pi^+\pi^-$ decay channels of the ρ^0 and ω mesons which are considered to produce coherently in the photo-induced reaction on the isoscalar nuclei. The distinctly dominant contribution to the cross section of the $\pi^0\gamma$ invariant mass distribution arises due to the $\omega \rightarrow \pi^0\gamma$ in the peak region. Therefore, the $\rho^0 \rightarrow \pi^0\gamma$ channel can be ignored for studying the physical phenomena associated with the ω meson (e.g., the modification of this meson in a nucleus) in the peak region. Few hundred MeV away from this region, the $\rho^0 \rightarrow \pi^0\gamma$ channel is very important because the contribution of this channel to the cross section is comparable to that of $\omega \rightarrow \pi^0\gamma$ channel. The cross section is also significantly increased in these regions due to the $\rho - \omega$ interference. Therefore, the cross section of the $\pi^0\gamma$ invariant mass distribution spectrum is drastically increased and the shape of it is remarkably changed due to ρ meson in the above mentioned regions of the spectrum. The cross section increases with the size of the nucleus and beam energy. The measureable cross section exits (specifically for the heavy nucleus and high energy) in the regions of $\pi^0\gamma$ invariant mass distribution spectrum where the contribution of the ρ meson and the $\rho - \omega$ interference is significant.

The spectrum calculated for the $\pi^+\pi^-$ invariant mass distribution due to ρ^0 meson reproduces the data reasonably well except in the ω meson peak region. The calculated

results show that the cross section because of the ω meson is insignificant compared to that due to the ρ meson. The cross section due to the $\rho^0 - \omega$ interference is significantly large at the pole mass of ω meson, resulting a sharp peak at this mass appearing in the $\pi^+\pi^-$ invariant mass distribution spectrum.

5 Acknowledgement

The author takes the opportunity to thank the anonymous referee for giving valuable comments which helped to improve the quality of the paper. Drs. A. Saxena and B. K. Nayak are gratefully acknowledged for their encouragement to work on the intermediate energy nuclear physics.

References

- [1] T. H. Bauer, R. D. Spital, D. R. Yennie and F. M. Pipkin, *Rev. Mod. Phys.* **50** (1978) 261; Erratum, *ibid*, **51** (1979) 407.
- [2] H. B. O'Connell, B. C. Pearce, A. W. Thomas and A. G. Williams, *Prog. Part. Nucl. Phys.* **39** (1997) 201.
- [3] H. Alvensleben et al., *Phys. Rev. Lett.* **25** (1970) 1373.
- [4] P. J. Biggs et al., *Phys. Rev. Lett.* **24** (1970) 1197.
- [5] M. F. M. Lutz and M. Soyeur, *Nucl. Phys. A* **760** (2005) 85.
- [6] C. Djalali et al., *Proceeding of Science (Hadron 2013)* 176.
- [7] H.-J. Behrend et al., *Phys. Rev. Lett.* **24** (1970) 336; H. Alvensleben et al., *Nucl. Phys. B* **18** (1970) 333.
- [8] P. J. Biggs et al., *Phys. Rev. Lett.* **24** (1970) 1201.
- [9] H.-J. Behrend et al., *Phys. Rev. Lett.* **27** (1971) 61.
- [10] H. Alvensleben et al., *Phys. Rev. Lett.* **27** (1971) 888.
- [11] S. Das, *Phys. Rev. C* **83** (2011) 064608.
- [12] S. Das, *Eur. Phys. J. A* **49** (2013) 123; A. Pautz and G. Shaw, *Phys. Rev. C* **57** (1998) 2648.

- [13] Ye. S. Golubeva, L. A. Kondratyuk and W. Cassing, Nucl. Phys. A **625** (1997) 832.
- [14] K. A. Olive et al., (Particle Data Group), Chin. Phys. C **38** (2014) 090001.
- [15] R. J. Glauber, in Lectures in theoretical physics, edited by W. E. Brittin et al., vol. 1 (Interscience Publishers, New York, 1959) p. 315; J. M. Eisenberg and D. S. Kolton, Theory of Meson Interaction with Nuclei (A Wiley-Interscience Publication, John Wiley & Sons, New York, 1980) p. 158.
- [16] S. Das, Phys. Rev. C **72** (2005) 064619; W. Peters, M. Post, H. Lenske, S. Leupold and U. Mosel, Nucl. Phys. A **632** (1998) 109; S. Das, Phys. Rev. C **78** (2008) 045210.
- [17] S. Das, Phys. Lett. B **737** (2014) 75; *ibid*, Phys. Rev. C **92** (2015) 014621.
- [18] L. A. Kondratyuk, A. Sibirtsev, W. Cassing, Ye. S. Golubeva and M. Effenberger, Phys. Rev. C **58** (1998) 1078.
- [19] A. Sibirtsev, Ch. Elster and J. Speth, arXiv:nucl-th/0203044.
- [20] G. I. Lykasov, W. Cassing, A. Sibirtsev and M. V. Ryzjanin, Eur. Phys. J. A **6** (1999) 71.
- [21] J. J. Sakurai, Currents and Mesons (The University of Chicago Press, Chicago, 1969) p. 48; R. K. Bhaduri, Models of the Nucleon (Addison-Wesley Publishing Company, Inc., California, 1988) p. 261.
- [22] A. Sibirtsev, H.-W. Hammer, U.-G. Meißner and A. W. Thomas, Eur. Phys. J. A **29** (2006) 209; A. Sibirtsev, H.-W. Hammer and U.-G. Meißner, Eur. Phys. J. A **37** (2008) 287.
- [23] R. M. Barnett et al., (Particle Data Group), Phys. Rev. D **54** (1996) 1; [<http://pdg.lbl.gov/xsect/contents.html>]
- [24] J. A. Gómez Tejedor and E. Oset, Nucl. Phys. A **600** (1996) 413.
- [25] C. W. De Jager, H. De Vries and C. De Vries, At. Data Nucl. Data Tables, **14** (1974) 479.
- [26] T. Ericson and W. Weise, Pions and Nuclei (Clarendon, Oxford, 1988) p. 36.

Figure Captions

1. (color online). The $\pi^0\gamma$ invariant mass m distribution spectra in the coherent (γ, V) reaction on ^{12}C nucleus. The enhancement in the cross section due to ρ^0 meson is distinctly visible beyond the peak region. See text for the explanation of various curves appearing in the figure.
2. (color online). Same as those presented in Fig. 1(b) but for the beam energy taken equal to 5 GeV.
3. (color online). Same as those presented in Fig. 2 but for ^{40}Ca nucleus.
4. (color online). The calculated $\pi^+\pi^-$ invariant mass m distribution spectra in the coherent (γ, V) reaction on ^{12}C nucleus. The data along with the background curves are taken from Ref. [10]. As mentioned in it, the background curves are due to the interference with non-resonant $\pi\pi$ emission (dot-dashed curve), the non-resonant $\pi\pi$ emission (dot-dot-dashed curve), and other background (large-dashed curve). The calculated results (added with the backgrounds) are compared with the data. The solid curve arises because of the contribution of the ω meson coherently added to that of the ρ^0 meson (short-dashed curve).
5. (color online). The calculated $\pi^+\pi^-$ invariant mass m distribution spectra originating due to the decay of ρ^0 and ω mesons photo-produced coherently in ^{12}C nucleus. Various curves appear in it are illustrated in the text.

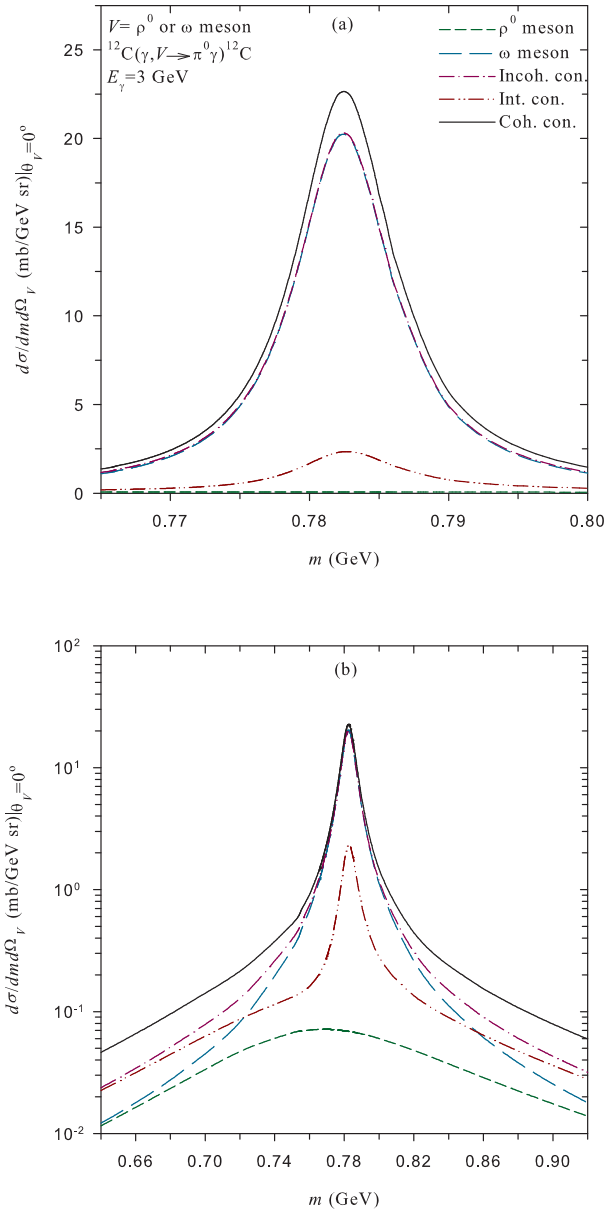


Figure 1: (color online). The $\pi^0\gamma$ invariant mass m distribution spectra in the coherent (γ, V) reaction on ^{12}C nucleus. The enhancement in the cross section due to ρ^0 meson is distinctly visible beyond the peak region. See text for the explanation of various curves appearing in the figure.

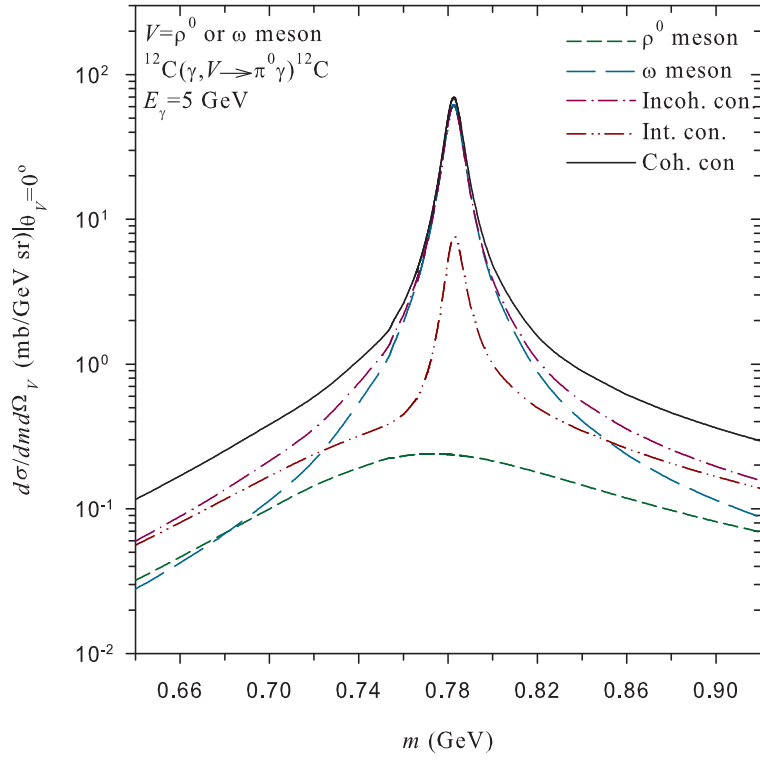


Figure 2: (color online). Same as those presented in Fig. 1(b) but for the beam energy taken equal to 5 GeV.

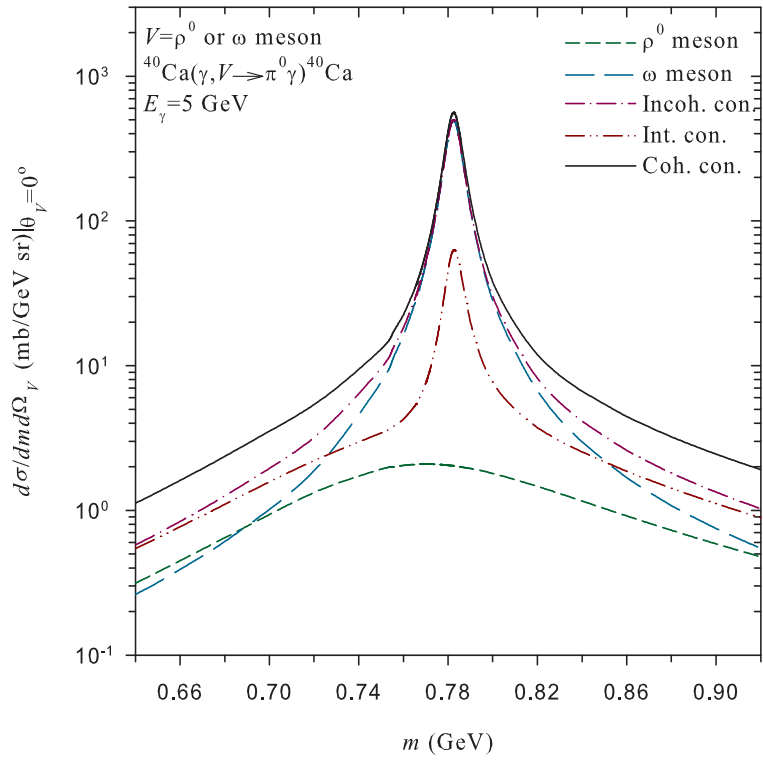


Figure 3: (color online). Same as those presented in Fig. 2 but for ^{40}Ca nucleus.

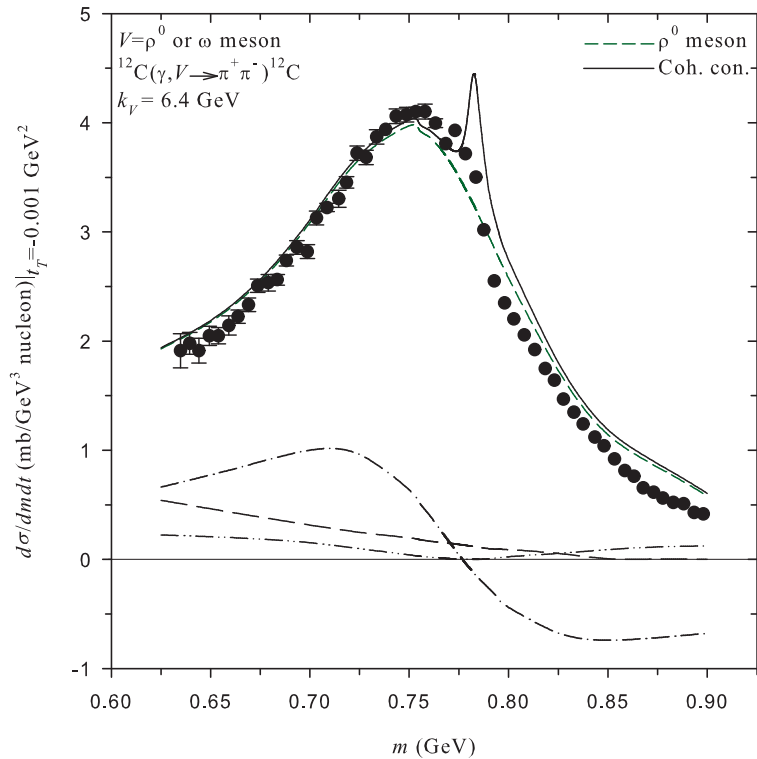


Figure 4: (color online). The calculated $\pi^+\pi^-$ invariant mass m distribution spectra in the coherent (γ, V) reaction on ^{12}C nucleus. The data along with the background curves are taken from Ref. [10]. As mentioned in it, the background curves are due to the interference with non-resonant $\pi\pi$ emission (dot-dashed curve), the non-resonant $\pi\pi$ emission (dot-dot-dashed curve), and other background (large-dashed curve). The calculated results (added with the backgrounds) are compared with the data. The solid curve arises because of the contribution of the ω meson coherently added to that of the ρ^0 meson (short-dashed curve).

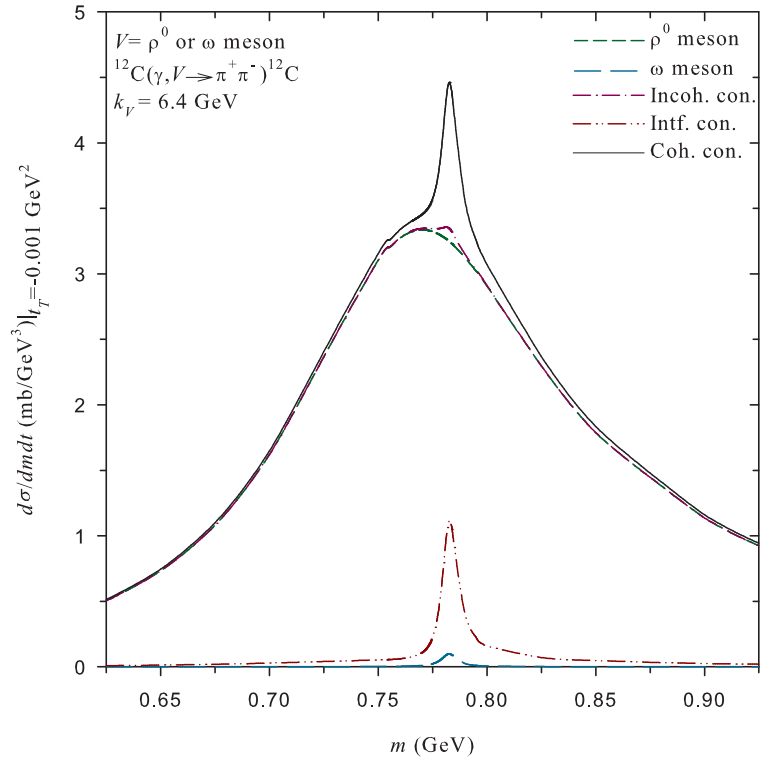


Figure 5: (color online). The calculated $\pi^+\pi^-$ invariant mass m distribution spectra originating due to the decay of ρ^0 and ω mesons photo-produced coherently in ^{12}C nucleus. Various curves appear in it are illustrated in the text.